

Article

Characterization of Hemp Hurd-Derived Biochar for Potential Agricultural Applications

Alberto Assirelli , Elisa Fischetti *, Antonio Scarfone * , Enrico Santangelo , Monica Carnevale , Enrico Paris , Adriano Palma  and Francesco Gallucci 

Council for Agricultural Research and Economics, Research Center for Engineering and Agro-Food Processing, Via della Pascolare 16, 00015 Monterotondo, RM, Italy; alberto.assirelli@crea.gov.it (A.A.); enrico.santangelo@crea.gov.it (E.S.); monica.carnevale@crea.gov.it (M.C.); enrico.paris@crea.gov.it (E.P.); adriano.palma@crea.gov.it (A.P.); francesco.gallucci@crea.gov.it (F.G.)

* Correspondence: elisa.fischetti@crea.gov.it (E.F.); antonio.scarfone@crea.gov.it (A.S.)

Abstract

Hemp (*Cannabis sativa* L.) is a high-yielding crop cultivated for fiber and seed production, generating substantial lignocellulosic residues such as hurds. These byproducts can be valorized through pyro-gasification, a thermochemical process that offers a sustainable alternative to combustion and produces biochar—a promising soil amendment due to its ability to enhance soil quality and mitigate drought stress. This research explores the viability of utilizing industrial hemp hurds as a direct feedstock for biochar production within the context of agricultural exploitation. The study specifically focuses on assessing the feasibility of converting raw, unprocessed hemp hurds into biochar through pyrolysis. A comprehensive characterization of the resulting biochar is conducted to evaluate its properties and potential applications in agriculture, establishing a foundational understanding for future agronomic use. Specific analysis included proximate and ultimate analysis, thermogravimetric analysis (TGA), SEM-EDS, and phytotoxicity testing. The biochar exhibited an alkaline pH (≥ 9), a low H/C ratio (0.37), and suitable macro- and micronutrient levels. Microstructural analysis revealed a porous architecture favorable for nutrient retention and water absorption. Germination tests with corn (*Zea mays* L.) showed a germination index above 90% for substrates containing 0.5–1% biochar. These findings establish a foundation for future research aimed at thoroughly exploring the agricultural potential of this material.

Keywords: biochar; hurd; fiber hemp; residue valorisation; agricultural applications; chemical composition; properties



Academic Editor: Huashou Li

Received: 30 July 2025

Revised: 1 September 2025

Accepted: 4 September 2025

Published: 5 September 2025

Citation: Assirelli, A.; Fischetti, E.; Scarfone, A.; Santangelo, E.; Carnevale, M.; Paris, E.; Palma, A.; Gallucci, F. Characterization of Hemp Hurd-Derived Biochar for Potential Agricultural Applications. *Agronomy* **2025**, *15*, 2136. <https://doi.org/10.3390/agronomy15092136>

Copyright: © 2025 by the authors. Licensee MDPI, Basel, Switzerland. This article is an open access article distributed under the terms and conditions of the Creative Commons Attribution (CC BY) license (<https://creativecommons.org/licenses/by/4.0/>).

1. Introduction

Among multipurpose crops, hemp (*Cannabis sativa* L.) has attracted notable scientific interest due to its rapid growth, high biomass yield, and adaptability to a wide range of climatic and soil conditions [1,2]. The species has a taproot system, classified as scapose therophyte, presenting an erect stem reaching 4 m height and a palmate leaf structure [3]. Genetic selection during the years allowed improving plant characteristics according to uses. According to variety, the plant can be monoecious or dioecious. In general, monoecious varieties are more suitable for the production of seeds, while dioecious are more suitable for the production of fibers [4,5]. Currently, monoecious French varieties such as Futura 75, Felina 32, and Fedora 17 are largely utilized in Europe as they provide good productions of both seeds and fiber, being considered multi-purpose crops [6,7].

Hemp seeds can be used for producing derivatives such as edible oil or flour. The nutritional and healthy properties of hemp seeds make the derivatives very appreciated by consumers and thoroughly researched in the elite food market [8]. However, the major use of hemp is recognized worldwide for the production of fibers obtained from the cortical part of the stems (bast fiber) [9]. Recently, the bast fibers gained importance also as renewable feedstock for the production of strong, lightweight composite material, offering several advantages as replacement for fiberglass [10]. Nowadays, the application of natural fiber composites are found in automotive interiors, agricultural and automotive exterior panels, acoustic and thermal insulation, furniture, recreational sport products such as tennis racquets, skateboards, and bike frames, marine products, and construction [11–14]. The hemp fibers are extracted through decortication processes which involve the use of specialized machines in different passages (scutching lines). The residue of the fiber processing consists of hurds and dust. The amount of residue generated from industrial processing of hemp can be considerable: different authors report that stem biomass in hemp cultivations yield between 7 and 8 t ha⁻¹ of dry matter [6,15,16]; the hurd portion represent about 70% of the total stem weight as reported in different studies [17,18], while dust represent a minimal fraction. Considering the great amount of hurd potentially obtainable from hemp cultivation, the recovery and valorization of this product may represent an opportunity requiring strong attention from different points of view. Hemp hurds have been already deeply studied and several commercial solutions are present in the global market. For instance, some authors studied the use of hurds for animal bedding, while others studied the use of hemp hurds for brick construction [18–20]. Among the various options, the syngas production through pyrolysis can be recognized as an effective and sustainable technique for valorizing the hemp residues [21]. The by-product of this process is biochar, a carbon-rich material that exhibits interesting physical and chemical characteristics for environmental and agronomic applications [22,23]. Usually, in order to efficiently produce synthetic gas and biochar for agriculture, different pyrolysis process modes are required. Indeed, pyrolysis product composition and yield depend on multiple factors, including biomass type, heating rate, vapor and solid residence times, temperature, reactor design, sample mass, and particle size and shape [24–26]. Biochar typically exhibits an alkaline pH, a notable presence of (hydroxy) iron oxides, a high specific surface area (high porosity), and various functional groups such as hydroxyl, ester, amine, carboxyl, and carbonyl [27]. These properties enable biochar to potentially act as a pollution controller for the removal of inorganic and organic contaminants, occurring through immobilization of the toxic components, thereby reducing their bioavailability and environmental dispersion [28]. Biochar is also an important material for environmental management to mitigate greenhouse gas emissions; the high number of micropores present in biochar has been successfully tested for the sequestration of CO₂, CH₄, and N₂O. Therefore, the interest in biochar has escalated in recent years, much owing to its well-documented capacity to sequester atmospheric carbon into soil [29,30].

In agriculture, the application of biochar demonstrates beneficial effects as a soil amendment, improving the soil's water holding capacity (WHC) and facilitating the storage of carbon, contributing to higher crop yields and mitigating the effect of droughts [31–33]. Microporosity and surface area are key factors influencing biochar's capacity to absorb and exchange nutrient ions, suggesting that smaller-particle biochar may enhance nutrient availability to plants [34]. The International Biochar Initiative defines high-quality biochar as a carbon-rich material produced via biomass pyrolysis, with growing interest in its potential to enhance agricultural sustainability and waste management [35].

Various biomass types can be used to obtain bioenergy and biochar; the largest part of the studies are dedicated to hardwood, softwood, or different types of residues [36,37].

Some studies already focused on hemp biochar, highlighting its biotechnological properties as carbon dioxide removal (CDR) material; among them, authors highlighted the high adsorption capacity, the soil carbon stability, and other multidisciplinary applications [38]. Some authors have pelletized and gasified hemp hurds mixed with sawdust, obtaining a biochar that was evaluated for agricultural applications [39]; other authors have ground and pelletized the entire stalks of hemp plants, obtaining a biochar composed of a mix of fibers, hurds, and dust tested as electrically conductive materials and solid biofuel [40]. Despite the interesting results obtained, pelletizing biomass is a laborious process that requires a grinding phase and a densification phase, with high energy consumption [41–43]. Additionally, grinding and densification are processes that alter the physical characteristics of the biomass and, consequently, can alter the final characteristics of the biochar [44]. The sustainability of using hemp hurds in thermochemical valorization processes should be sought in the direct use of this material derived from industrial processes; in this regard, a lack of studies focused on the characterization of hemp hurd biochar for agricultural applications resulting directly from fiber industrial processing was identified. Avoiding the pre-processing of biomass would be a sustainable way to valorize this agricultural residue, but the feasibility of a direct conversion should be thoroughly investigated with respect to chemical and physical properties of the product obtained. Firstly, this study aimed at evaluating the feasibility of a direct biochar conversion from unprocessed hemp hurds. Secondly, the work was focused on the characterization of the biochar derived from hemp hurds through the analysis of various chemical and physical aspects of this material, which represent the baseline for agricultural applications.

2. Materials and Methods

2.1. Feedstock

The start material consisted of 100 air-dried hemp stems obtained from a plantation of the Futura 75 variety, cultivated at the Bergonzini farm in Bondeno (Ferrara, Italy), harvested in August 2023. All stems were characterized by measuring diameter (by means of a caliber) and height. Then, the stems were laid on concrete surface and crushed with an agricultural roller repeatedly to resemble the effect of rollers present in fiber scutching lines as verified in different preliminary tests. Successively, manual decortication was performed to separate the bast fibers from the woody core (hurds) in order to obtain a raw hemp hurd matrix (Figure 1).



Figure 1. Hemp stems (a), hemp hurds (b).

As a standard methodology for the classification of such material is missing, the residues were grouped in height and diametric classes practically chosen according to minimum and maximum dimensions identified. The main dimensional classes chosen for the classification are shown in Table 1.

Table 1. Dimensional classification of hemp stems and hemp hurds.

Hemp Stem		Hemp Hurd
Diameter Class (mm)	Length Class (cm)	Length Class (cm)
$2 < x < 4$	$90 < x < 100$	$25 < x < 40$
$4 < x < 6$	$100 < x < 110$	$41 < x < 55$
$6 < x < 8$	$110 < x < 120$	$56 < x < 70$
$8 < x < 10$	$120 < x < 130$	$70 < x < 80$

The characterization of hemp hurd biomass and biochar was performed at LASER-B Lab (Laboratory of Experimental Activities and Renewable Energy from Biomass) of CREA-IT in Monterotondo, Rome. The chemical characterization of the hurds prior to conversion were described separately by Assirelli et al. (2024) [45]. In addition, in the present work, the hemp hurd biomass was characterized with respect to dimensional analysis (length of 100 pieces), volatile matter (VM), fixed carbon (FC), and thermogravimetric analysis (TGA) to provide a more complete view of chemical and physical characteristics of the start material. The determination of the volatile matter content was carried out on a dry basis by using 1 g of minced hemp hurds in three replicates; the material was put in a crucible and inserted in a muffle furnace (mod. Lenton EF11/8B, Lenton, Hope Valley, United Kingdom) at 925 ± 10 °C for 7 min according to ASTM D 3175-89 [46]. The fixed carbon was determined by the difference between 100% and moisture content, ash content, and volatiles.

The thermogravimetric analysis (TGA) aims to measure the phase variation of the mass sample subjected to a temperature rate into a controlled atmosphere. The METTLER TGA/DSC1 STAR was used to measure the degradation kinetics simulating the pyrolysis process of hemp hurds to simulate the pyrolysis conditions. TGA was carried out using a minced sample of 5.2 mg, with N₂ used as gas carrier at 100 mL min⁻¹ and with a heating rate of 35 °C min⁻¹ up to a final temperature of 525 °C maintained for 15 min [40].

2.2. Pyrolysis, Biochar Production, and Characterization

The pyrolysis process was carried out with a prototype pyro-gasifier made by DIMA (Department of Mechanical and Aerospace Engineering-Sapienza University of Rome, Rome, Italy), used in previous studies [30,45,47], with some structural adjustments of the fluidized bed gasifier to make it suitable for a fixed-bed pyrolysis. Table 2 reports the operative conditions applied which largely influenced the yield of the various products.

Table 2. Pyrolysis operative conditions.

Parameter	
Biomass	80 g
N ₂ flow	5 NL min ⁻¹
Reactor temperature	550 °C
Pyrolysis time	25 min
Heating rate	21 °C min ⁻¹

The pyrolysis process leads to the formation of three main products, one for each state of matter:

- Liquid (tars, bio-oil, and water);
- Solid (biochar and ash);
- Gas (syngas).

The yields of each by-product have been calculated to define a mass balance. Among the values reported in Table 2, the value of temperature (550 °C) was chosen to balance a small latency due to the electric resistance placed inside the reactor, which may result in some differential degrees (lower) in the core of the biomass during pyro-gasification. This setup enabled us to achieve the temperature of the process closely matching the one simulated during TGA. The following calculations were made to determine the syngas produced during pyrolysis. In the pyrolysis process like that of the present study, at 500–600 °C, the syngas yield (S_y) can be approximated to 60% of the volatile fraction [48]. The volatile fraction (V_f) was determined from volatile matter (VM%) using Equation (1) [46]:

$$V_f = \text{Biomass (g)} \cdot \frac{(\text{VM}\%)}{100} \cdot \frac{(100 - \text{Moisture } \%)}{100}. \quad (1)$$

The amount of syngas produced was determined according to Equation (2), considering that the average density of syngas of $0.9 \text{ g} \cdot \text{L}^{-1}$ [49].

$$\text{Syngas (L)} = \frac{V_f \cdot S_y}{S_d} \quad (2)$$

where S_y is the syngas yield and S_d is the syngas density. After estimating the amount of syngas produced and knowing the biomass input and the residual biochar, it was possible to determine by difference the quantity of condensable products (bio-oil, tar, etc.). At the end of the process, after cooling, biochar samples (Figure 2) were collected and characterized.



Figure 2. Hemp biochar produced after the pyrolysis process.

As for hemp biomass, the length of 100 pieces of biochar was measured using a caliber. Chemical characterization included elemental analysis, metal content determination, and pH measurement. The elemental content (C, H, N, S, O) of biochar was determined by using a Costech ECS 4010 CHNS–O (Valencia, CA, USA) elemental analyzer according to UNI EN ISO 16948:2015 [50]. Atomic H:C and O:C ratios were determined starting from elemental composition.

For the determination of metal content, the samples were homogenized and mineralized. Then, the samples (about 0.5 g each) were prepared through weighing by adding $6 \pm 0.1 \text{ mL}$ of HNO_3 65% and $3 \pm 0.1 \text{ mL}$ of H_2O_2 30% by using a microwave Milestone START D (Milestone srl, Sorisole (BG), Italy) according to the U.S. EPA Method 3051A. After the dilution the samples were analyzed by ICP-MS (Agilent 7700, Agilent Technologies, Santa Clara, CA, USA) according to UNI EN ISO 16967:2015 [51] and UNI EN ISO 16968:2015 [52], the pH was measured in a solution prepared with deionized water (50 mL)

and about 5 g of sample using the Eutech Instruments (Eutech Instruments Pte Ltd, Singapore) pH700 pH/mV/°C/°F Bench Meter with a glass electrode, according to UNI EN 13037:2012 [53].

The morphology, the structure, the surface characteristics, the identification, and the quantification of the chemical elements were carried out by using SEM Zeiss EVO MA 10 + EDS Bruker Quantax 200 (Carl Zeiss S.p.A, Milan, Italy). SEM analysis coupled with EDS gives information on the chemical composition of the biochar, which is in turn influenced by the dynamics of the conversion process [54] and the composition of the biomass used [55].

2.3. Germination Test

Germination tests were conducted on corn (*Zea mays* L.) seeds to test the degree of toxicity of different concentrations of biochar according to guideline ISO 17126:2024 [56]. Three concentrations of aqueous extracts from hemp hurd biochar were compared: 0.5, 1, and 5% (W/v).

The resulting amount of substrate was weighed, dissolved in 40 mL of distilled water and left for 24 h in the dark at room temperature. The supernatant was filtered on a double-layered gauze and freeze-stored in Falcon tubes until use. The experiment was performed in triplicate, and for each replicate, seven seeds of corn were sown in Petri dishes (15 cm diameter). The capsules were incubated in the dark at 24 °C for four days when germination percentages were assessed. The following traits were analyzed: number of germinated seeds, number of secondary roots, epicotyl length, and hypocotyl length.

In addition, the germination index (GI) was calculated according to the following Equation (3) [56]:

$$GI \% = \left[\frac{(Gc * Lc)}{(Gt * Lt)} \right] * 100 \quad (3)$$

where

Gc = mean number of germinated seeds from the treatment;

Lc = average radical length of treatment (cm);

Gt = mean number of germinated seeds of the control;

Lt = average radical length of the control (cm).

2.4. Statistical Analysis

The data of the germination test were analyzed with the software Jamovi 2.2.5 (a graphical interface of R version 1.6, "<https://jamovi.org> (accessed on 5 June 2025)". They were checked for normality and, once their deviation from normality was verified, subjected to the Kruskal–Wallis test for non-parametric ANOVA.

3. Results and Discussions

3.1. Biomass Characterization

The hemp stems were relatively short compared to the average length of hemp stalks traditionally grown (Tables 3 and 4). This is because the apical parts of the plant were already removed during seed harvesting and the portion considered represents the fraction without flowering parts, which is commonly used for fiber production when hemp is cultivated as a multipurpose crop [57,58]. Hurd pieces were between 25 and 80 mm, largely below 50 mm. This data is in line with outputs from patented machineries, which showed that the length of industrial hurd falls predominantly between 1 and 5 cm, with common values around 15–30 mm "<https://canadiangreenfield.com/hemptrain/> (accessed on 15 July 2025)"; "<https://hurdmaster.com/> (accessed on 15 July 2025)"; "<https://formation-ag.com/products/processing/decorticator/fibertrack660> (accessed on 15 July 2025)".

Table 3. Hemp stem dimensional analysis.

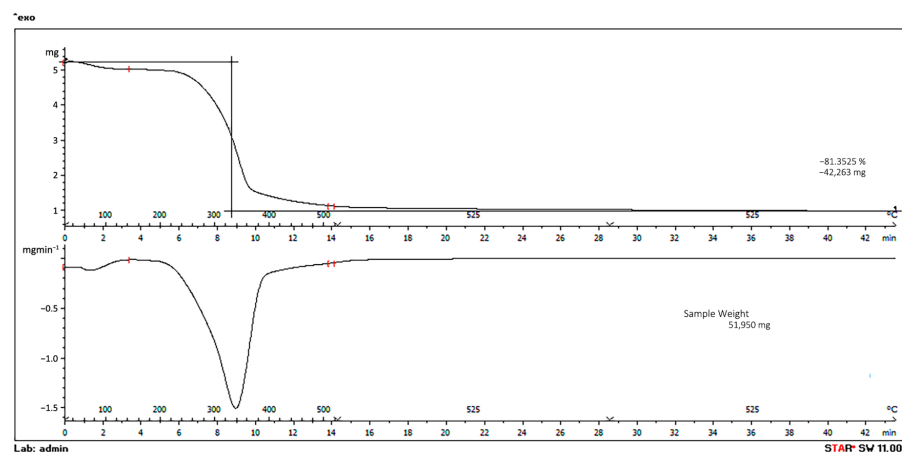
Hemp Stem			
Diameter Class (mm)	Number of Pieces	Length Class (cm)	Number of Pieces
2 < x < 4	9	90 < x < 100	36
4 < x < 6	57	100 < x < 110	47
6 < x < 8	24	110 < x < 120	15
8 < x < 10	10	120 < x < 130	2

Table 4. Hemp hurd dimensional analysis.

Hemp Hurd	
Length Class (cm)	Number of Pieces
25 < x < 40	44
41 < x < 55	39
56 < x < 70	13
70 < x < 80	4

Considering the preliminary results published by Assirelli et al. (2024) [45], the chemical composition of the hemp hurds was similar to that of wood biomass, with a moderately high carbon content (45.17%), low amounts of hydrogen (5.25%), and low nitrogen content (0.45%). Similar values are reported in studies on woody biomasses displaying a carbon content between 45% and 50% (pine, oak, elm, eucalyptus, and poplar biomasses). The main difference compared to traditional lignocellulosic biomass was the heating value and the ash content, with results lower and higher than that of other woody biomass, respectively [59,60]. Volatile matter was equal to $70.60 \pm 0.82\%$, while fixed carbon was $10.81 \pm 0.72\%$.

The simulation of pyrolysis showed a mass loss of about 4.23 mg, corresponding to 80% of the starting material (Figure 3). Thermal decomposition suggested that at low temperature (about 100 °C), the mass loss was due to dehydration followed by the degradation of the fibers such as hemicellulose, cellulose, and lignin. Specifically, hemicellulose starts to decompose between 200 and 300 °C, while cellulose decomposes between 300 and 400 °C; on the other hand, lignin has a broad decomposition temperature range, with significant degradation occurring between 250 and 500 °C. The biochar produced from hemp hurds demonstrated a similar thermogravimetric decay to that of other biomass [61,62]. Once 500 °C is reached, 80% of the biomass degrades thermally, with the residual fraction being mainly composed of ash, char, and to a small extent residual lignin.

**Figure 3.** Hemp thermal degradation.

3.2. Biochar Characterization

The carbon content of hemp hurd biochar was above 75% (Table 5). The value is higher than the percentage reported for biochar produced from other herbaceous biomasses. Jung et al. (2008) [63] and Mansaray and Ghaly (1997) [64] observed 40% and 52% of carbon content in biochar of rice and wheat straw, respectively. Values similar to hemp hurds have been reported for woody biomasses like eucalyptus, acacia, and pine [65]. Although the nitrogen (N) content was very low, the results for potassium (K), carbon (C), and pH suggest good potential for agricultural applications. The alkaline pH of hemp biochar indicates the potential of this material to correct acidic soils, while the C/N ratio greater than 30 indicates the ability to slow down the degradation processes of organic matter [66,67].

Table 5. Chemical characterization of hemp hurds and hemp hurd biochar.

Parameters	Hemp Hurd *	Hemp Hurd Biochar
C%	45.71 ± 0.68	76.22 ± 4.66
H%	5.25 ± 0.77	2.36 ± 0.32
N%	0.45 ± 0.13	0.97 ± 0.10
S%	2.17 ± 0.03	0.55 ± 0.07
O%	42.07 ± 1.74	19.89 ± 4.44
pH	-	9.63 ± 0.05
H:C	-	0.37
O:C	-	0.19

* Values from Assirelli et al. 2024 [45].

The values of H:C and O:C were very low. These ratios provide insights about aromaticity, environmental stability, resistance to microbial degradation, and carbonization. The O:C values below 0.4 suggest low oxidation during pyrolysis, affecting the final product's polarity and water retention ability [68]. The molar ratios comply with the limits set by the European Biochar Foundation and align with other studies on pyrolysis of herbaceous biomass, showing similar results at the same operating conditions [69,70].

Regarding macro- and microelements (Tables 6 and 7), the analysis displays a high content of Ca, Mg, and K, indicating the formation of metal oxides, which are able to influence the alkalinity of the material [71]. In fact, the biochar obtained displayed a highly alkaline pH; this is also influenced by factors such as the temperature reached during pyrolysis, the carbonization process, and the nature of the feedstock [72]. Using alkaline biochar as a soil amendment helps to increase soil alkalinity, affecting phenomena such as the availability and mobility of metals, the degradation of organic matter, and the sequestration of essential nutrients for plant growth [73]. Table 6 lists the minor elements contained within the biochar. The heavy metal content in the biochar was below the legal set limits (DL 75/2010) for all elements [74].

Table 6. Concentrations of major elements in hemp hurd biochar.

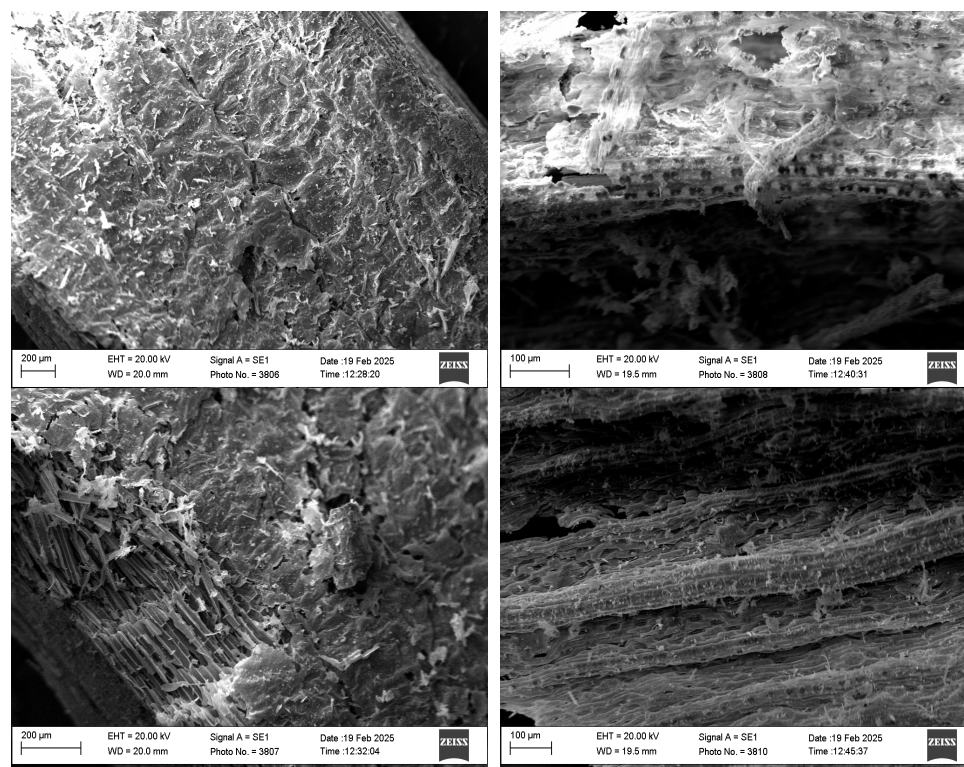
	Macro-Elements (g kg ⁻¹)
Na	0.36 ± 25.00
Mg	2.34 ± 91.42
K	18.23 ± 245.05
Ca	2.88 ± 17.68

Table 7. Concentrations of micronutrients and trace elements in hemp hurd biochar.

	Micro-Elements (mg kg ⁻¹)
B	86.46 ± 5.05
Cr	0.54 ± 3.41
Mn	334.52 ± 29.73
Fe	3683.10 ± 236.65
Co	2.34 ± 0.35
Ni	16.49 ± 2.08
Cu	33.55 ± 5.77
Zn	143.97 ± 47.66
Al	221.63 ± 56.2
As	2.85 ± 0.78
Mo	1.33 ± 0.57
Ag	0.20 ± 0.06
Cd	0.17 ± 0.03
Sn	2.19 ± 0.81
Ba	13.96 ± 1.25
Pb	1.02 ± 0.11

3.3. Qualitative and Quantitative Analysis with SEM-EDS

Shown below are the images concerning the microstructure of the hemp hurd biochar (Figure 4). The morphology of hemp biochar appears compact and with a physical structure characterized by pores, with dimensions comparable to biochar from woody biomass (Figure 5). The micropores displayed dimensions between 15 and 30 µm, comparable with that of poplar. The phenomena of pore formation is due to the expulsion of volatile compounds, which in turn is influenced by the characteristics of the raw material and pyrolysis conditions [75].

**Figure 4.** SEM image of hemp biochar.

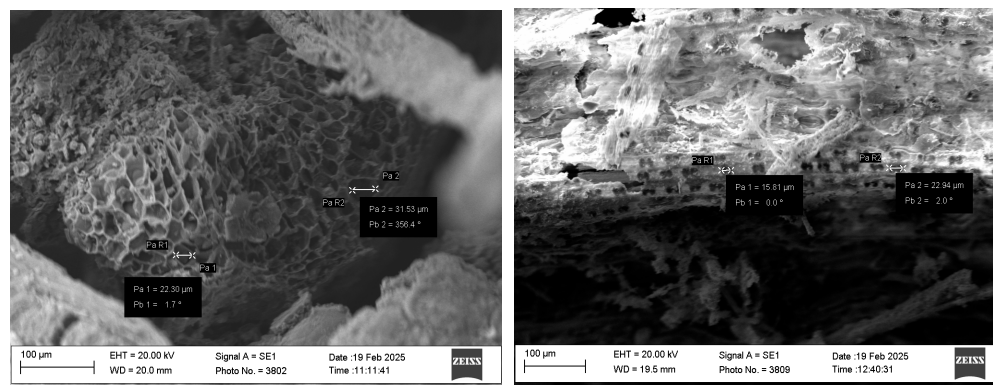


Figure 5. SEM images and pores dimension of poplar (left) and hemp hurd biochar (right).

Another important element affecting the surface area and the volume of the micropores of the biochar is the size of the start material; these physical factors generally increase as the size of the material decreases [76]. In fact, finer biomass particles, having a larger surface area for heat exchange within the reactor, induce the formation of larger diameter pores from which volatile matter is released [77,78]. Results of dimensional analysis are displayed in Table 8. More than half (65%) of the biochar was between 30 and 50 mm, with a thickness never above 0.5 cm. In general, the overall dimension and the volume of singular hemp hurd biochar particles were much lower with respect to that of woody biomasses (Figure 6).

Table 8. Hemp hurd biochar dimensional analysis.

Dimensional Classes (mm)	n. Pieces
23–30	13
31–40	36
41–50	29
51–60	12
61–72	10

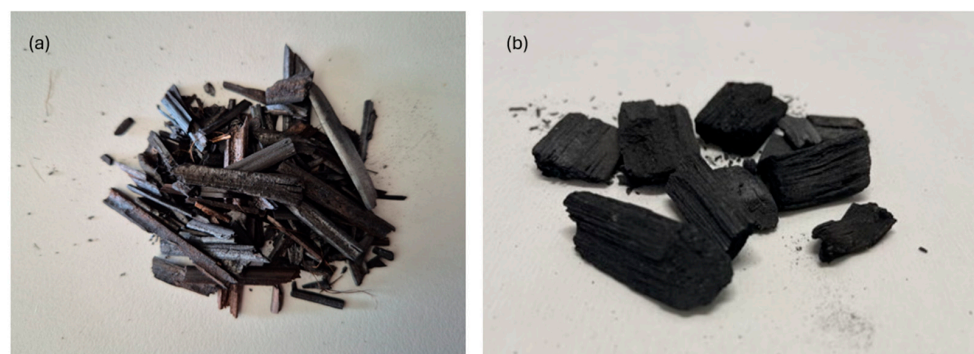


Figure 6. Images of poplar biochar (a) and hemp biochar (b).

From a simple visual observation, the hemp hurd biochar was clearly lower in size and less homogeneous than that of poplar. The micropores structure and fine fractions present in hemp hurd biochar suggests positive implications for agricultural applications such as high WHC, high nutrient retention capacity, optimal interaction with soil microorganisms, and greater susceptibility to their attacks [79]. However, it must be stressed that several factors such as the soil's physical and chemical properties, the characteristics of the biochar [54,55], the type of feedstock used [80], and the carbon content of the biochar may affect these properties [81,82]. For instance, the particle size and the porous structure of the biochar

may influence the WHC of the material. As studied by Wang et al., 2019 [83], biochar with a high surface area and particle sizes of 1–2 mm can temporarily increase field capacity in sandy soils, while its effects are limited in clay soils. Additionally, Xie et al. (2015) [84] highlighted that smaller particles enhance the absorption of nutrients and organic compounds. According to Sun et al. (2012) [85], reducing the particle size of the feedstock increases the microporosity of the resulting biochar. Other studies confirm that finer particles exhibit larger Brunauer–Emmett–Teller (BET) surface areas [84,86]. However, the increase in water holding capacity (WHC) is primarily driven by the biochar application rate and soil type [87].

Figure 7 and Table 9 show the results of the energy-dispersive X-ray spectroscopy (EDS). It highlighted the presence of elements such as carbon, potassium, oxygen, and aluminum. The qualitative and quantitative analysis by EDS confirmed the results obtained from the analysis of metal content in ICP-MS. Similar studies on hemp stalks confirmed the presence of elements such as O, C, K, and Al on the surface analyzed, also including elements such as Ca and Cl [40]. In general, the presence of these elements indicates the formation of compounds such as K_2O and Al_2O_3 within the biochar.

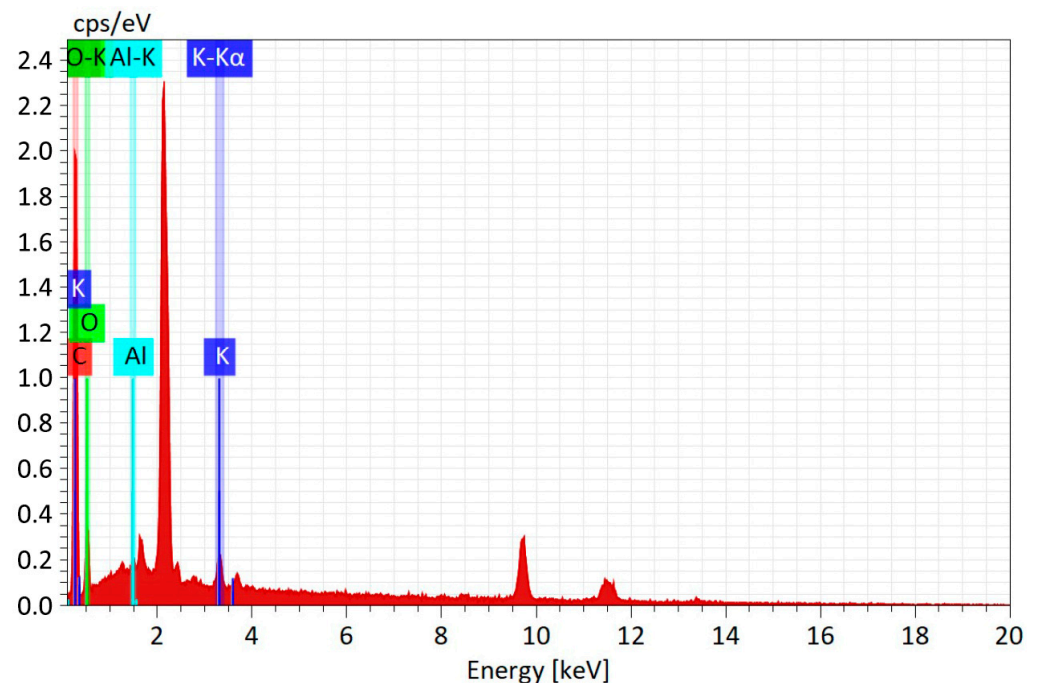


Figure 7. EDS graph of hemp biochar.

Table 9. Chemical elements of hemp biochar identified with the EDS analysis.

Element	Mass%
C	94.28
K	3.19
O	1.54
Al	0.99

3.4. Pyrolysis and By-Products Yields

According to Equation (1) and the experimentally determined VM% (Section 2.2), V_f is equal to the following:

$$V_f = Biomass (g) \cdot \frac{(VM\%)}{100} \cdot \frac{(100 - Moisture \%)}{100} = 80 \cdot \frac{70.60}{100} \cdot \frac{(100 - 18.41)}{100} = 46.08 g. \tag{4}$$

By entering the data in Equation (2), the number of liters of syngas obtained from the pyrolysis process can be determined:

$$\text{Syngas (L)} = \frac{V_f \cdot S_y}{S_d} = \frac{46.08 \text{ g} \cdot 0.6}{0.9 \left(\frac{\text{g}}{\text{L}}\right)} = \frac{27.65 \text{ g}}{0.9 \left(\frac{\text{g}}{\text{L}}\right)} = 30.72 \text{ L.} \quad (5)$$

By knowing the amount of biochar at the end of the process, the initial amount of fresh biomass, and the amount of syngas produced, it is possible to determine by difference the quantity of condensable products (bio-oil, tar, water, etc.):

$$\text{Liquid (g)} = \text{Biomass (g)} - \text{Syngas (g)} - \text{Biochar (g)} = 80 - 27.64 - 32.2 = 20.15 \text{ g.} \quad (6)$$

Therefore, the percentage distribution of pyrolysis products is as follows:

Liquid (tars, bio-oil, and water) = 25.2%;

Solid (biochar and ash) = 40.3%;

Gas (syngas) = 34.6%.

There is a lack of literature on pyro-gasification balance of pure hemp hurd biomass. However, for solid production, the results obtained tend to be in line with those of other woody biomass (40.3% for hemp hurds vs. 40% other woody biomass), while for liquid and gas production the values result respectively lower (25.2% for hemp hurds vs. 38% other woody biomass) and higher (34.6% for hemp hurds vs. 22% other woody biomass) [88].

In a study conducted by Marrot et al. (2022) [40], the hemp stalks of Futura 75 hemp variety were minced, pelletized, and gasified to obtain a biochar for electrical applications. Similarly to the present work, these authors performed a chemical analysis on the biochar and a TGA of the biomass. In the closest conditions of our study, with low temperature and slow pyrolysis process (P600-R200-T30), the results obtained concerning N, H, C, and H/C were similar to our findings, while values of O (3.7 vs. 19.9) and O/C (0.03 vs. 0.19) differed remarkably. This difference may be due the “atmosphere” of pyrolysis, influencing the presence of O during the process, or the residual moisture present in biomass. However, it must be pointed out that the original biomass in the study of Marrot et al. (2022) [40] was the whole stem, including the bast fiber of the plant. This may have influenced the presence of certain chemical elements. The behavior of the biomass in TGA for the two studies was comparable, with degradations of hemicellulose and cellulose occurring between 200 and 400 °C, and degradation of lignin between 250 and 500 °C.

Thanks to its high biomass productivity—reaching up to 20 t·ha^{−1} of fresh biomass under optimal cultivation conditions [89]—and considering the final energy balance of the hurd gasification processing, industrial hemp shows promising potential for energy production.

3.5. Results on Germination Test

Table 10 shows the absence of statistical significance for the number of germinated seeds (*p* value = 0.521), hypocotyl length (*p* value = 0.064), number of radicles (*p* value = 0.555), and epicotyl length (*p* value = 0.078).

Table 10. Statistics of the Kruskal–Wallis test on the germination data (*p* < 0.05).

	χ^2	df	<i>p</i>
N° of germinated seeds	2.26	3	0.521
Epicotyl length (cm)	7.26	3	0.064
N° of secondary rootlets	2.09	3	0.555
Epicotyl length (cm)	6.81	3	0.078

The seed germination index (GI) was proposed for evaluating the toxicity of compost, but it can also give valuable information for other growing substrates [90,91]. Values between 30% and 80% of the germinability index generally indicate possible phytotoxicity while values above 80% indicate that the substance has no phytotoxic effect [87]. Data from aqueous extract of hemp biochar (Figure 8) showed that the germination index decreases significantly as the concentration of biochar increases. GI dropped from 104% to 59% as the biochar concentration increased from 0.5 to 5%. It should be noted that the highest biochar concentration (5%) resulted in a GI of 59%, a value that falls within the range (30–80%) suggestive of potential phytotoxicity.

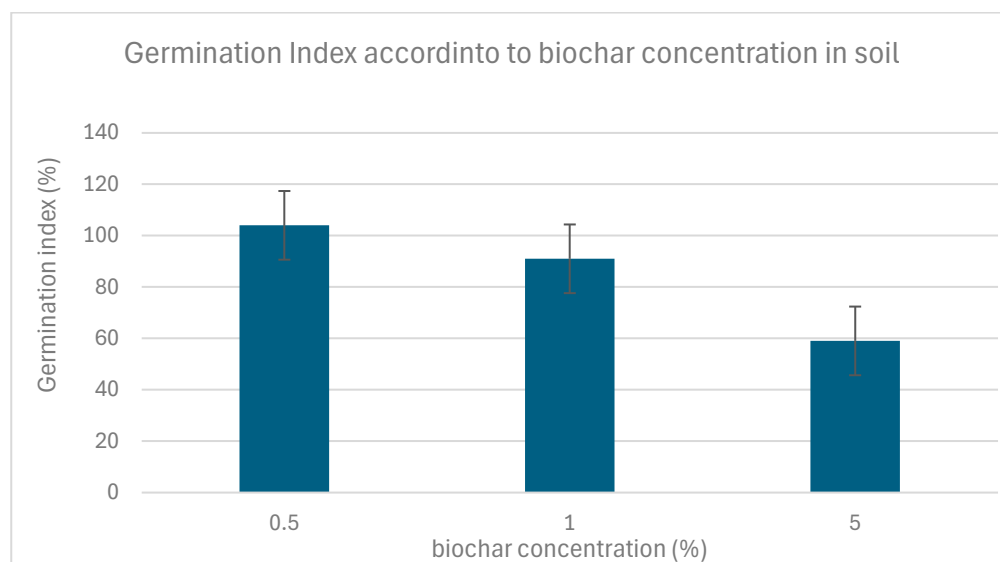


Figure 8. Germination index of corn seeds using different concentrations of hemp hurd biochar.

Although the goal of our study was not assessing the effect of pyrolysis temperature of hemp biochar, the literature evidence indicates that higher pyrolysis or gasification temperatures generally reduce phytotoxicity and improve germination outcomes (e.g., *Lepidium sativum* germinability tests—best results with high-temperature or gasification biochars) [39].

Research on other feedstocks (e.g., wheat, corn) shows that biochar extracts from lower-temperature pyrolysis (approx. 300 °C) can completely inhibit germination, while higher-temperature biochars (around 400 °C) allow ~69% germination and healthier seedling growth [92]. Moreover, phytotoxic compounds such as Polycyclic Aromatic Hydrocarbons (PAHs), phenolics, or volatile organic compounds present in biochar extracts have been identified as responsible for seedling inhibition—washing the biochar mitigates these toxic effects [93].

In light of our findings—namely a decrease in germination index from 104% to 59% as hemp biochar concentration increased—the observed phytotoxicity may be influenced by residual toxic compounds in the biochar produced at a temperature of 550 °C. These results align with patterns seen in the existing literature. Future studies should include characterization of biochar production parameters (especially pyrolysis temperature) and consider washing treatments to reduce potential toxicity.

4. Conclusions

The use of hemp as a biomass source for energy production has gained significant interest within the circular economy framework, especially when hemp is used as multipurpose crop. Based on the results obtained, the hemp hurd-derived biochar directly

obtainable from industrial defibering processes (no pre-processing needed) demonstrated favorable characteristics for use as a soil amendment, including high carbon content and the presence of essential nutrients. In particular, the results revealed that the biochar meets regulatory standards, with low concentrations of heavy metals, an alkaline pH (≥ 9), a hydrogen-to-carbon (H/C) ratio of 0.37, and with acceptable levels of macro- and micronutrients.

The germination tests using corn seeds (*Zea mays* L.) was the baseline to verify the potential for agricultural use; this was confirmed with good perspectives considering the germination index above 90% for substrates containing 0.5% to 1% of biochar.

In conclusion, the findings of this paper offer insights for the valorization of hemp hurd biomass with an ecological perspective, giving the baseline for testing future agronomic applications in the fields of phytotoxicity, soil fertility, and water retention.

Author Contributions: All authors contributed to the study conception and design. Material preparation, data collection, and analysis were performed by M.C., E.P., A.P., F.G., and E.F. M.C., E.S., E.F., A.S., A.A., and E.P. contributed to the writing and modifications. A.A. contributed to the acquisition of funding. A.S., A.A., and E.S. contributed to the revision. All authors have read and agreed to the published version of the manuscript.

Funding: The work was supported by the Italian Ministry of Agriculture, Food Sovereignty and Forests (MASAF) under the CARIFIT project (D.D. n. 0667575 on 30 December 2022).

Data Availability Statement: The datasets generated during and/or analyzed during the current study are available from the corresponding author on reasonable request.

Conflicts of Interest: The authors declare no conflicts of interest.

Abbreviations

The following abbreviations are used in this manuscript:

BET	Brunauer–Emmett–Teller
CREA-IT	Council for Agricultural Research and Economics, Research Center for Engineering and Agro-Food processing
CDR	Carbon Dioxide Removal
DIMA	Department of Mechanical and Aerospace Engineering-Sapienza University of Rome
FC	Fixed Carbon
SEM-EDS	Scanning Electron Microscope-Energy-Dispersive X-ray Spectroscopy
TGA	Thermogravimetric Analyzer
VM	Volatile Matter
WHC	Water Holding Capacity

References

- Baldini, M.; Ferfuaia, C.; Piani, B.; Sepulcri, A.; Dorigo, G.; Zuliani, F.; Danuso, F.; Cattivello, C. The Performance and Potentiality of Monoecious Hemp (*Cannabis sativa* L.) Cultivars as a Multipurpose Crop. *Agronomy* **2018**, *8*, 162. [[CrossRef](#)]
- Rehman, M.; Fahad, S.; Du, G.; Cheng, X.; Yang, Y.; Tang, K.; Liu, L.; Liu, F.-H.; Deng, G. Evaluation of Hemp (*Cannabis sativa* L.) as an Industrial Crop: A Review. *Environ. Sci. Pollut. Res. Int.* **2021**, *28*, 52832–52843. [[CrossRef](#)] [[PubMed](#)]
- Fidan, M.; Süzerer, V.; Onay, A. *Cannabis sativa* L.: Origin, Distribution, Taxonomy and Biology. *Türk Bilimsel Derlemeler Derg.* **2023**, *16*, 10–28.
- Petit, J.; Salentijn, E.M.J.; Paulo, M.-J.; Denneboom, C.; Trindade, L.M. Genetic Architecture of Flowering Time and Sex Determination in Hemp (*Cannabis sativa* L.): A Genome-Wide Association Study. *Front. Plant Sci.* **2020**, *11*, 569958. [[CrossRef](#)]
- Salentijn, E.M.J.; Zhang, Q.; Amaducci, S.; Yang, M.; Trindade, L.M. New Developments in Fiber Hemp (*Cannabis sativa* L.) Breeding. *Ind. Crops Prod.* **2015**, *68*, 32–41. [[CrossRef](#)]
- Tang, K.; Struik, P.C.; Yin, X.; Thouminot, C.; Bjelková, M.; Stramkale, V.; Amaducci, S. Comparing Hemp (*Cannabis sativa* L.) Cultivars for Dual-Purpose Production under Contrasting Environments. *Ind. Crops Prod.* **2016**, *87*, 33–44. [[CrossRef](#)]

7. Tang, K.; Struik, P.C.; Yin, X.; Calzolari, D.; Musio, S.; Thouminot, C.; Bjelková, M.; Stramkale, V.; Magagnini, G.; Amaducci, S. A Comprehensive Study of Planting Density and Nitrogen Fertilization Effect on Dual-Purpose Hemp (*Cannabis sativa* L.) Cultivation. *Ind. Crops Prod.* **2017**, *107*, 427–438. [CrossRef]
8. Tănase Apetroaei, V.; Pricop, E.M.; Istrati, D.I.; Vizireanu, C. Hemp Seeds (*Cannabis sativa* L.) as a Valuable Source of Natural Ingredients for Functional Foods—A Review. *Molecules* **2024**, *29*, 2097. [CrossRef]
9. Pari, L.; Baraniecki, P.; Kaniewski, R.; Scarfone, A. Harvesting Strategies of Bast Fiber Crops in Europe and in China. *Ind. Crops Prod.* **2015**, *68*, 90–96. [CrossRef]
10. Iucolano, F.; Boccarusso, L.; Langella, A. Hemp as Eco-Friendly Substitute of Glass Fibres for Gypsum Reinforcement: Impact and Flexural Behaviour. *Compos. Part B Eng.* **2019**, *175*, 107073. [CrossRef]
11. Dayo, A.Q.; Luengrojankul, P.; Boonao, N.; Charoensuk, K.; Argunam, H.; Ahn, C.-H.; Rimdusit, S. Development of Flame Retardant and Thermally Stable Acoustic Green Composites from Waste Hemp Fibers Reinforcement in Fully Biobased Epoxy and Benzoxazine Hybrid Thermosets. *Int. J. Lightweight Mater. Manuf.* **2024**, *8*, 658–668. [CrossRef]
12. Gencil, O.; Güler, O.; Ustaoglu, A.; Erdoğmuş, E.; Sari, A.; Hekimoğlu, G.; Boztoprak, Y.; Subaşı, S. Characteristics of Cement-Based Thermo-Concretes Containing Capric Acid Impregnated Hemp for Thermal Energy Storage and Sound Isolation in Buildings. *Energy* **2025**, *329*, 136837. [CrossRef]
13. Nawawithan, N.; Kittisakpairach, P.; Nithiboonyapun, S.; Ruangjirakit, K.; Jongpradist, P. Design and Performance Simulation of Hybrid Hemp/Glass Fiber Composites for Automotive Front Bumper Beams. *Compos. Struct.* **2024**, *335*, 118003. [CrossRef]
14. Umair, M.; Khan, R.M.W.U. Fibers for Sports Textiles. In *Fibers for Technical Textiles*; Ahmad, S., Rasheed, A., Nawab, Y., Eds.; Springer International Publishing: Cham, Switzerland, 2020; pp. 93–115. ISBN 978-3-030-49224-3.
15. Baldini, M.; Ferfuia, C.; Zuliani, F.; Danuso, F. Suitability Assessment of Different Hemp (*Cannabis sativa* L.) Varieties to the Cultivation Environment. *Ind. Crops Prod.* **2020**, *143*, 111860. [CrossRef]
16. Carus, M.; Meridionale, C.; Kauffmann, A.; Hobson, J.; Bertucelli, S. The European Hemp Industry: Cultivation, Processing and Applications for Fibres, Shives and Seeds. Available online: <https://pdf.sciencedirectassets.com/271144/1-s2.0-S0926669016X00052/1-s2.0-S0926669016302436/main.pdf?X-Amz-Security-T> (accessed on 3 June 2025).
17. Dudzic, P.; Warmiński, K.; Stolarski, M.J. Industrial Hemp As a Multi-Purpose Crop: Last Achievements and Research in 2018–2023. *J. Nat. Fibers* **2024**, *21*, 2369186. [CrossRef]
18. Kołodziej, J.; Kicińska-Jakubowska, A. Utilization of Hemp Shives for Various Purposes—A Review. *J. Nat. Fibers* **2025**, *22*, 2448016. [CrossRef]
19. Borhan, M.D.S.; Rahman, S.; Hammer, C. Water Absorption Capacity of Flax and Pine Horse Beddings and Gaseous Concentrations in Bedded Stalls. *J. Equine Vet. Sci.* **2014**, *34*, 611–618. [CrossRef]
20. Small, E.; Marcus, D. *Hemp: A New Crop with New Uses for North America*; Reprinted from: Trends in New Crops and New, Uses; Janick, J., Whipkey, A., Eds.; ASHS Press: Alexandria, VA, USA, 2002.
21. del Carmen Recio-Ruiz, M.; Ruiz-Rosas, R.; García-Mateos, F.J.; Valero-Romero, M.J.; Rosas, J.M.; Rodríguez-Mirasol, J.; Cordero, T. An Integrated Approach to the Valorization of Pyrolysis Products from Lignocellulosic Residues and By-Products. *Biomass Bioenergy* **2025**, *196*, 107676. [CrossRef]
22. Amalina, F.; Syukor Abd Razak, A.; Krishnan, S.; Sulaiman, H.; Zularisam, A.W.; Nasrullah, M. Advanced Techniques in the Production of Biochar from Lignocellulosic Biomass and Environmental Applications. *Clean. Mater.* **2022**, *6*, 100137. [CrossRef]
23. Zhu, X.; Labianca, C.; He, M.; Luo, Z.; Wu, C.; You, S.; Tsang, D.C.W. Life-Cycle Assessment of Pyrolysis Processes for Sustainable Production of Biochar from Agro-Residues. *Bioresour. Technol.* **2022**, *360*, 127601. [CrossRef]
24. Tiwari, M.; Dirbeba, M.J.; Lehmusto, J.; Yrjas, P.; Vinu, R. Analytical and applied pyrolysis of challenging biomass feedstocks: Effect of pyrolysis conditions on product yield and composition. *J. Anal. Appl. Pyrolysis* **2024**, *177*, 106355. [CrossRef]
25. Jerzak, W.; Acha, E.; Li, B. Comprehensive Review of Biomass Pyrolysis: Conventional and Advanced Technologies, Reactor Designs, Product Compositions and Yields, and Techno-Economic Analysis. *Energies* **2024**, *17*, 5082. [CrossRef]
26. Li, X.; Lu, Y.; Liu, P.; Wang, Z.; Huhe, T.; Chen, Z.; Wu, Y.; Lei, T. A Study on the Pyrolysis Behavior and Product Evolution of Typical Wood Biomass to Hydrogen-Rich Gas Catalyzed by the Ni-Fe/HZSM-5 Catalyst. *Catalysts* **2024**, *14*, 200. [CrossRef]
27. Sohi, S.P.; Krull, E.; Lopez-Capel, E.; Bol, R. A Review of Biochar and Its Use and Function in Soil. In *Advances in Agronomy*; Elsevier: Amsterdam, The Netherlands, 2010; Volume 105, pp. 47–82. ISBN 978-0-12-381023-6.
28. Pinna, M.V.; Lauro, G.P.; Diquattro, S.; Garau, M.; Senette, C.; Castaldi, P.; Garau, G. Softwood-Derived Biochar as a Green Material for the Recovery of Environmental Media Contaminated with Potentially Toxic Elements. *Water Air Soil Pollut.* **2022**, *233*, 152. [CrossRef]
29. Atkinson, C.J.; Fitzgerald, J.D.; Hipps, N.A. Potential Mechanisms for Achieving Agricultural Benefits from Biochar Application to Temperate Soils: A Review. *Plant Soil* **2010**, *337*, 1–18. [CrossRef]
30. Gallucci, F.; Palma, A.; Vincenti, B.; Carnevale, M.; Paris, E.; Ancona, V.; Migliarese Caputi, M.V.; Borello, D. Fluidized Bed Gasification of Biomass from Plant Assisted Bioremediation (PABR): Lab-Scale Assessment of the Effect of Different Catalytic Bed Material on Emissions. *Fuel* **2022**, *322*, 124214. [CrossRef]

31. Abideen, Z.; Koyro, H.-W.; Huchzermeyer, B.; Ansari, R.; Zulfiqar, F.; Gul, B. Ameliorating Effects of Biochar on Photosynthetic Efficiency and Antioxidant Defence of Phragmites Karka under Drought Stress. *Plant Biol.* **2020**, *22*, 259–266. [[CrossRef](#)]
32. Hansen, V.; Müller-Stöver, D.; Ahrenfeldt, J.; Holm, J.K.; Henriksen, U.B.; Hauggaard-Nielsen, H. Gasification Biochar as a Valuable By-Product for Carbon Sequestration and Soil Amendment. *Biomass Bioenergy* **2015**, *72*, 300–308. [[CrossRef](#)]
33. Hansen, V.; Müller-Stöver, D.; Imparato, V.; Krogh, P.H.; Jensen, L.S.; Dolmer, A.; Hauggaard-Nielsen, H. The Effects of Straw or Straw-Derived Gasification Biochar Applications on Soil Quality and Crop Productivity: A Farm Case Study. *J. Environ. Manag.* **2017**, *186*, 88–95. [[CrossRef](#)]
34. Liao, W.; Thomas, S.C. Biochar Particle Size and Post-Pyrolysis Mechanical Processing Affect Soil pH, Water Retention Capacity, and Plant Performance. *Soil Syst.* **2019**, *3*, 14. [[CrossRef](#)]
35. Lehmann, J.; Joseph, S. (Eds.) *Biochar for Environmental Management: Science, Technology and Implementation*, 2nd ed.; Routledge: London, UK, 2015; ISBN 978-0-203-76226-4.
36. Ajiën, A.; Idris, J.; Md Sofwan, N.; Husen, R.; Seli, H. Coconut Shell and Husk Biochar: A Review of Production and Activation Technology, Economic, Financial Aspect and Application. *Waste Manag. Res.* **2023**, *41*, 37–51. [[CrossRef](#)] [[PubMed](#)]
37. Seow, Y.X.; Tan, Y.H.; Mubarak, N.M.; Kandedo, J.; Khalid, M.; Ibrahim, M.L.; Ghasemi, M. A Review on Biochar Production from Different Biomass Wastes by Recent Carbonization Technologies and Its Sustainable Applications. *J. Environ. Chem. Eng.* **2022**, *10*, 107017. [[CrossRef](#)]
38. Wang, Z.; Li, T.; Song, B.; Liu, S.; Li, S. Thermochemical Conversion of Waste Hemp Textiles into Hierarchical Porous Carbons for CO₂ Capture: Kinetic Insights and Structure–Property Relationships. *AIP Adv.* **2025**, *15*, 055107. [[CrossRef](#)]
39. Puglia, M.; Morselli, N.; Lumi, M.; Santunione, G.; Pedrazzi, S.; Allesina, G. Assessment of Hemp Hurd-Derived Biochar Produced through Different Thermochemical Processes and Evaluation of Its Potential Use as Soil Amendment. *Heliyon* **2023**, *9*, e14698. [[CrossRef](#)]
40. Marrot, L.; Candelier, K.; Valette, J.; Lanvin, C.; Horvat, B.; Legan, L.; DeVallance, D.B. Valorization of Hemp Stalk Waste Through Thermochemical Conversion for Energy and Electrical Applications. *Waste Biomass Valor.* **2022**, *13*, 2267–2285. [[CrossRef](#)]
41. Bergman, R.D.; Zhang, H.; Englund, K.; Windell, K.; Gu, H. Estimating GHG Emissions from the Manufacturing of Field-Applied Biochar Pellets. In Proceedings of the 59th International Convention of Society of Wood Science and Technology, Curitiba, Brazil, 6–10 March 2016; pp. 1–11.
42. Bergman, R.; Sahoo, K.; Englund, K.; Mousavi-Avval, S.H. Lifecycle Assessment and Techno-Economic Analysis of Biochar Pellet Production from Forest Residues and Field Application. *Energies* **2022**, *15*, 1559. [[CrossRef](#)]
43. Mohammadi, A. Overview of the Benefits and Challenges Associated with Pelletizing Biochar. *Processes* **2021**, *9*, 1591. [[CrossRef](#)]
44. Gutiérrez, J.; Rubio-Clemente, A.; Pérez, J.F. Analysis of Biochars Produced from the Gasification of Pinus Patula Pellets and Chips as Soil Amendments. *Maderas. Cienc. Tecnol.* **2022**, *24*. [[CrossRef](#)]
45. Assirelli, A.; Fischetti, E.; Santangelo, E.; Civitarese, V.; Palma, A.; Vincenti, B.; Salerno, M.; Paris, E.; Carnevale, M.; Gallucci, F. Technical and Energetic Characterization of the Different Products Obtainable from Industrial Hemp. In Proceedings of the European Biomass Conference and Exhibition Proceedings 2024, 32nd EUBCE-Marseille 2024, Marseille, France, 24–29 June 2024; pp. 582–586. [[CrossRef](#)]
46. ASTM D 3175-89; Standard Test Method for Volatile Matter in the Analysis Sample of Coal and Coke. ASTM International: West Conshohocken, PA, USA, 1989; p. 305.
47. Gallucci, F.; Paris, E.; Palma, A.; Vincenti, B.; Carnevale, M.; Ancona, V.; Borello, D. Fluidized Bed Gasification of Biomass from Plant-Assisted Bioremediation: Fate of Contaminants. *Sustain. Energy Technol. Assess.* **2022**, *53*, 102458. [[CrossRef](#)]
48. Demirbas, A. Pyrolysis of Biomass for Fuels and Chemicals. *Energy Sources Part A Recovery Util. Environ. Eff.* **2009**, *31*, 1028–1037. [[CrossRef](#)]
49. Mustafa, A.; Calay, R.K.; Mustafa, M.Y. A Techno-Economic Study of a Biomass Gasification Plant for the Production of Transport Biofuel for Small Communities. *Energy Procedia* **2017**, *112*, 529–536. [[CrossRef](#)]
50. UNI EN ISO 16948:2015; Solid Biofuels—Determination of Total Content of Carbon, Hydrogen and Nitrogen. ISO: Geneva, Switzerland, 2015.
51. UNI EN ISO 16967:2015; Solid Biofuels—Determination of Major Elements—Al, Ca, Fe, Mg, P, K, Si, Na and Ti. ISO: Geneva, Switzerland, 2015.
52. UNI EN ISO 16968:2015; Solid Biofuels—Determination of Minor Elements. ISO: Geneva, Switzerland, 2015.
53. UNI EN 13037:2012; Soil Improvers and Growing Media—Determination of pH. ISO: Geneva, Switzerland, 2012.
54. Hassan, M.; Liu, Y.; Naidu, R.; Parikh, S.J.; Du, J.; Qi, F.; Willett, I.R. Influences of Feedstock Sources and Pyrolysis Temperature on the Properties of Biochar and Functionality as Adsorbents: A Meta-Analysis. *Sci. Total Environ.* **2020**, *744*, 140714. [[CrossRef](#)]
55. Wiersma, W.; Van Der Ploeg, M.J.; Sauren, I.J.M.H.; Stoof, C.R. No Effect of Pyrolysis Temperature and Feedstock Type on Hydraulic Properties of Biochar and Amended Sandy Soil. *Geoderma* **2020**, *364*, 114209. [[CrossRef](#)]

56. ISO 17126:2024(En); Soil Quality—Determination of the Effects of Pollutants on Soil Flora—Screening Test for Emergence of Lettuce Seedlings (*Lactuca sativa* L.). ISO: Geneva, Switzerland, 2024. Available online: <https://www.iso.org/obp/ui/en/#iso:std:iso:17126:ed-2:v1:en> (accessed on 19 May 2025).
57. Amaducci, S.; Zatta, A.; Pelatti, F.; Venturi, G. Influence of Agronomic Factors on Yield and Quality of Hemp (*Cannabis sativa* L.) Fibre and Implication for an Innovative Production System. *Field Crops Res.* **2008**, *107*, 161–169. [CrossRef]
58. Musio, S.; Müssig, J.; Amaducci, S. Optimizing Hemp Fiber Production for High Performance Composite Applications. *Front. Plant Sci.* **2018**, *9*, 1702. [CrossRef]
59. Nordin, A. Chemical Elemental Characteristics of Biomass Fuels. *Biomass Bioenergy* **1994**, *6*, 339–347. [CrossRef]
60. Wongsiriamnuay, T.; Tippayawong, N. Thermogravimetric Analysis of Giant Sensitive Plants under Air Atmosphere. *Bioresour. Technol.* **2010**, *101*, 9314–9320. [CrossRef] [PubMed]
61. Di Blasi, C. Modeling Chemical and Physical Processes of Wood and Biomass Pyrolysis. *Prog. Energy Combust. Sci.* **2008**, *34*, 47–90. [CrossRef]
62. Ferdous, D.; Dalai, A.K.; Bej, S.K.; Thring, R.W. Pyrolysis of Lignins: Experimental and Kinetics Studies. *Energy Fuels* **2002**, *16*, 1405–1412. [CrossRef]
63. Jung, S.-H.; Kang, B.-S.; Kim, J.-S. Production of Bio-Oil from Rice Straw and Bamboo Sawdust under Various Reaction Conditions in a Fast Pyrolysis Plant Equipped with a Fluidized Bed and a Char Separation System. *J. Anal. Appl. Pyrolysis* **2008**, *82*, 240–247. [CrossRef]
64. Mansaray, K.G.; Ghaly, A.E. Agglomeration Characteristics of Alumina Sand-Rice Husk Ash Mixtures at Elevated Temperatures. *Energy Sources* **1997**, *19*, 1005–1025. [CrossRef]
65. González-Prieto, Ó.; Ortiz Torres, L.; Vazquez Torres, A. Comparison of Waste Biomass from Pine, Eucalyptus, and Acacia and the Biochar Elaborated Using Pyrolysis in a Simple Double Chamber Biomass Reactor. *Appl. Sci.* **2024**, *14*, 1851. [CrossRef]
66. Dai, Z.; Zhang, X.; Tang, C.; Muhammad, N.; Wu, J.; Brookes, P.C.; Xu, J. Potential Role of Biochars in Decreasing Soil Acidification—A Critical Review. *Sci. Total Environ.* **2017**, *581*, 601–611. [CrossRef]
67. Malabadi, R.B.; Kolkar, K.P.; Chalannavar, R.K.; Acharya, M.; Mudigoudra, B.S. Industrial Cannabis Sativa-Hemp: Biochar Applications and Disadvantages. *World J. Adv. Res. Rev.* **2023**, *20*, 371–383. [CrossRef]
68. Conte, P.; Schmidt, H.-P.; Cimò, G. Research and Application of Biochar in Europe. In *SSSA Special Publications*; Guo, M., He, Z., Uchimiya, S.M., Eds.; American Society of Agronomy and Soil Science Society of America: Madison, WI, USA, 2015; pp. 409–422. ISBN 978-0-89118-967-1.
69. Saikia, R.; Chutia, R.S.; Kataki, R.; Pant, K.K. Perennial Grass (*Arundo donax* L.) as a Feedstock for Thermo-Chemical Conversion to Energy and Materials. *Bioresour. Technol.* **2015**, *188*, 265–272. [CrossRef]
70. Zheng, H.; Wang, Z.; Deng, X.; Zhao, J.; Luo, Y.; Novak, J.; Herbert, S.; Xing, B. Characteristics and Nutrient Values of Biochars Produced from Giant Reed at Different Temperatures. *Bioresour. Technol.* **2013**, *130*, 463–471. [CrossRef]
71. DeLuca, T.H.; Gundale, M.J.; MacKenzie, M.D.; Jones, D.L. Biochar Effects on Soil Nutrient Transformations. In *Biochar for Environmental Management*; Routledge: Oxford, UK, 2015; ISBN 978-0-203-76226-4.
72. Cheng, H.; Jones, D.L.; Hill, P.; Bastami, M.S.; Tu, C. long Influence of Biochar Produced from Different Pyrolysis Temperature on Nutrient Retention and Leaching. *Arch. Agron. Soil Sci.* **2018**, *64*, 850–859. [CrossRef]
73. Baronti, S.; Vaccari, F.P.; Miglietta, F.; Calzolari, C.; Lugato, E.; Orlandini, S.; Pini, R.; Zulian, C.; Genesio, L. Impact of Biochar Application on Plant Water Relations in *Vitis vinifera* (L.). *Eur. J. Agron.* **2014**, *53*, 38–44. [CrossRef]
74. Saracini, C. Decreto Legislativo 75/2010. Disciplina Fertilizzanti—Consolidato. Available online: <https://www.certifico.com/haccp/264-legislazione-chemicals-food/15653-decreto-legislativo-75-2010-disciplina-fertilizzanti-consolidato> (accessed on 23 May 2025).
75. Braghiroli, F.L.; Bouafif, H.; Neculita, C.M.; Koubaa, A. Influence of Pyro-Gasification and Activation Conditions on the Porosity of Activated Biochars: A Literature Review. *Waste Biomass Valor.* **2020**, *11*, 5079–5098. [CrossRef]
76. Fahmi, A.H.; Samsuri, A.W.; Jol, H.; Singh, D. Physical Modification of Biochar to Expose the Inner Pores and Their Functional Groups to Enhance Lead Adsorption. *RSC Adv.* **2018**, *8*, 38270–38280. [CrossRef]
77. Liu, R.; Liu, G.; Yousaf, B.; Abbas, Q. Operating Conditions-Induced Changes in Product Yield and Characteristics during Thermal-Conversion of Peanut Shell to Biochar in Relation to Economic Analysis. *J. Clean. Prod.* **2018**, *193*, 479–490. [CrossRef]
78. Mui, E.L.K.; Cheung, W.H.; McKay, G. Tyre Char Preparation from Waste Tyre Rubber for Dye Removal from Effluents. *J. Hazard. Mater.* **2010**, *175*, 151–158. [CrossRef] [PubMed]
79. Leng, L.; Xiong, Q.; Yang, L.; Li, H.; Zhou, Y.; Zhang, W.; Jiang, S.; Li, H.; Huang, H. An Overview on Engineering the Surface Area and Porosity of Biochar. *Sci. Total Environ.* **2021**, *763*, 144204. [CrossRef]
80. Huang, H.; Reddy, N.G.; Huang, X.; Chen, P.; Wang, P.; Zhang, Y.; Huang, Y.; Lin, P.; Garg, A. Effects of Pyrolysis Temperature, Feedstock Type and Compaction on Water Retention of Biochar Amended Soil. *Sci. Rep.* **2021**, *11*, 7419. [CrossRef]
81. Liu, P.; Zhu, M.; Zhang, Z.; Leong, Y.-K.; Zhang, Y.; Zhang, D. Rheological Behaviour and Stability Characteristics of Biochar-Water Slurry Fuels: Effect of Biochar Particle Size and Size Distribution. *Fuel Process. Technol.* **2017**, *156*, 27–32. [CrossRef]

82. Sun, F.; Lu, S. Biochars Improve Aggregate Stability, Water Retention, and Pore-Space Properties of Clayey Soil. *J. Plant Nutr. Soil Sci.* **2014**, *177*, 26–33. [[CrossRef](#)]
83. Wang, D.; Li, C.; Parikh, S.J.; Scow, K.M. Impact of Biochar on Water Retention of Two Agricultural Soils—A Multi-Scale Analysis. *Geoderma* **2019**, *340*, 185–191. [[CrossRef](#)]
84. Xie, T.; Reddy, K.R.; Wang, C.; Yargicoglu, E.; Spokas, K. Characteristics and Applications of Biochar for Environmental Remediation: A Review. *Crit. Rev. Environ. Sci. Technol.* **2015**, *45*, 939–969. [[CrossRef](#)]
85. Sun, H.; Hockaday, W.C.; Masiello, C.A.; Zygourakis, K. Multiple Controls on the Chemical and Physical Structure of Biochars. *Ind. Eng. Chem. Res.* **2012**, *51*, 3587–3597. [[CrossRef](#)]
86. Valenzuela-Calahorra, C.; Bernalte-García, A.; Gómez-Serrano, V.; Bernalte-García, M.J. Influence of Particle Size and Pyrolysis Conditions on Yield, Density and Some Textural Parameters of Chars Prepared from Holm-Oak Wood. *J. Anal. Appl. Pyrolysis* **1987**, *12*, 61–70. [[CrossRef](#)]
87. Zhang, J.; Amonette, J.E.; Flury, M. Effect of Biochar and Biochar Particle Size on Plant-Available Water of Sand, Silt Loam, and Clay Soil. *Soil Tillage Res.* **2021**, *212*, 104992. [[CrossRef](#)]
88. Basu, P. *Biomass Gasification, Pyrolysis and Torrefaction: Practical Design and Theory*; Academic Press: Cambridge, MA, USA, 2018; ISBN 978-0-12-813040-7.
89. Pari, L.; Alfano, V.; Scafone, A. An innovative harvesting system for multipurpose hemp. In Proceedings of the 24th European Biomass Conference and Exhibition, Amsterdam, The Netherlands, 6–9 June 2016; pp. 356–358.
90. Luo, Y.; Liang, J.; Zeng, G.; Chen, M.; Mo, D.; Li, G.; Zhang, D. Seed Germination Test for Toxicity Evaluation of Compost: Its Roles, Problems and Prospects. *Waste Manag.* **2018**, *71*, 109–114. [[CrossRef](#)]
91. Beesigamukama, D.; Subramanian, S.; Tanga, C.M. Nutrient Quality and Maturity Status of Frass Fertilizer from Nine Edible Insects. *Sci. Rep.* **2022**, *12*, 7182. [[CrossRef](#)]
92. Kataya, G.; El Charif, Z.; Badran, A.; Cornu, D.; Bechelany, M.; Hijazi, A.; Sukkariyah, B.; Issa, M. Evaluating the impact of different biochar types on wheat germination. *Sci. Rep.* **2024**, *14*, 28663. [[CrossRef](#)] [[PubMed](#)]
93. Rogovska, N.; Laird, D.; Cruse, R.M.; Trabue, S.; Heaton, E. Germination tests for assessing biochar quality. *J. Environ. Qual.* **2012**, *41*, 1014–1022. [[CrossRef](#)] [[PubMed](#)]

Disclaimer/Publisher’s Note: The statements, opinions and data contained in all publications are solely those of the individual author(s) and contributor(s) and not of MDPI and/or the editor(s). MDPI and/or the editor(s) disclaim responsibility for any injury to people or property resulting from any ideas, methods, instructions or products referred to in the content.